Methylhydrosilyl Chemostructural Effects in Polyhydrosilanes

Liviu Sacarescu,*,† Angeliki Siokou,‡ Gabriela Sacarescu,† Mihaela Simionescu,† and Ionel Mangalagiu§

Inorganic Polymers Department, Institute of Macromolecular Chemistry "Petru Poni", Aleea Gr. Ghica Voda 41A, 700487, Iasi, Romania, Foundation of Research and Technology Hellas, Institute of Chemical Engineering and High Temperature Chemical Processes (FORTH/ICE-HT), Stadiou Str. Platani Achaias, P.O. Box 1414, Rion, GR-26504, Patras, Greece, and Organic Chemistry Department, "Al. I. Cuza" University, Bd. Carol 11, 700506, Iasi, Romania

Received August 16, 2007; Revised Manuscript Received November 9, 2007

ABSTRACT: The presence of the methylhydrosilyl segments within the poly(diphenylsilane) chain lead to important conformational changes and the formation of elemental silicon particles. To investigate these processes polyhydrosilanes with various contents of methylhydrosilyl groups were synthesized by homogeneous coupling of methyldichlorosilane with diphenyldichlorosilane. Spectral analysis techniques combined with atomic force and polarized light microscopy were used to elucidate the mechanism of the silicon particle formation within the polymeric matrix.

Introduction

In recent years, intense research has been dedicated to the modification of a wide variety of material properties simply by reducing the material domain size in order to obtain quantum non-negligible effects. Semiconductors have been the subject of the majority of this work, particular attention being paid to silicon. Silicon quantum size effects have been exploited to investigate properties such as photoluminescence,[1] melting and sintering,[2] band gap energy,[3] physical strength of derivative ceramics,[4] and phosphorescence.[5] Due to the importance of silicon in modern technology, modifications of its properties have a major impact on leading industrial sectors including electronics, aerospace, computers, energy, and sensors.

Polysilanes are well-known merely as precursors for silicon carbide[6] and their exploitation as a possible source for optoelectronic materials is just beginning. Research in this field proved that UV irradiation or thermal processing of polysilanes under certain conditions, leads to a slight enrichment in elemental silicon especially when the material is deposited as a thin layer.[7,8] This property could be useful as a different approach to obtain polycrystalline silicon structures and layers by taking advantage of specially designed highly reactive soluble oligo- and polysilanes.

This work presents the chemostructural effects induced by methylhydrosilyl groups enclosed within a poly(diphenylsilane) chain. It is shown that this specific structure is capable of producing small particles of elemental silicon with controllable dimension and possesses a long-ordered helical conformation with extended σ-electron delocalization.

Discussion

Polyhydrosilane structures with various reactive methylhydrosilyl contents studied within this work were prepared by low-temperature homogeneous Wurtz coupling of diphenyldichlorosilane with controlled amounts of methyldichlorosilane. The homogeneous reaction system was obtained using THF solutions of crown ethers sodium metal complexes. The corresponding specific mechanism ensures a high molecular weight monomodal distribution avoiding destruction of the Si−H reactivity through side reactions[9] (Supporting Information Scheme S1). The composition of the resulted poly[diphenylsilane-*co*-methyl(H)-silane] (PDPHS) was controlled by selection of the CH_3HSiCl_2/$(C_6H_5)_2SiCl_2$ monomers ratios as 1/1 (a-PDPHS), 1/7 (b-PDPHS), and 1/20 (c-PDPHS).[9] To obtain comparative results, a poly(methylphenylsilane) homopolymer (PMPS) was prepared by the same procedure.

The spectral characterization showed the specific details related to the synthesized polyhydrosilanes and confirms their chemical structures. Besides their functionality, the Si−H groups within the poly(diphenylsilane) backbone induced some intriguing effects.

Conformational Effects of the Methylhydrosilyl Segments. The conformational effects of the methylhydrosilyl fragments appeared when polysilanes were investigated by fluorescence spectroscopy (FL). First, it was observed that the FL spectral profile of PMPS with a full width at half-maximum, fwhm = 25 nm, is very different from the mirror image of the absorption band at 340 nm indicating that the stiff helical chain conformation of PMPS has frequent irregularities (Figure 1).[10]

In contrast, a-PDPHS shows relatively narrow UV absorptions with fwhm = 15 nm, and the FL spectral profile is closer to the mirror image of the 350 nm absorption band. This is somehow surprising because the fragmentation of the polysilane chain due to the high content of small methyl(H)silyl segments should produce a UV absorption maximum shift to lower wavelengths, widening of the bands and strong irregularities in the FL spectra.[10,11] The absence of such effects indicates that the long diphenylsilyl segments with a stiff and regular helical global conformation[11] are coupled through trans-planar flexible fragments which eliminate the internal conformational tensions inducing a highly ordered polymeric structure. The same conclusion could be drawn from the powder X-ray diffraction (XRD) analysis (Figure 2a).

† Inorganic Polymers Department, Institute of Macromolecular Chemistry "Petru Poni".

‡ Foundation of Research and Technology Hellas, Institute of Chemical Engineering and High Temperature Chemical Processes (FORTH/ICE-HT).

§ Organic Chemistry Department, "Al. I. Cuza" University.

* Corresponding author. Telephone: +40 232 217454. Fax: +40 232 211299. E-mail: livius@icmpp.ro.

10.1021/ma071853f CCC: $40.75
Published on Web 01/03/2008

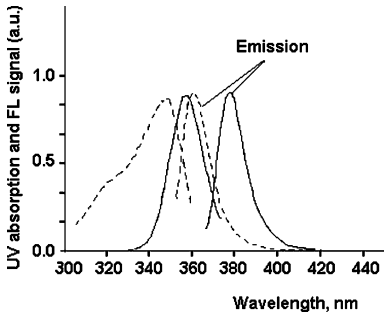

Figure 1. Absorption and Emission Spectra of PMPS (dotted) and a-PDPHS (continuous).

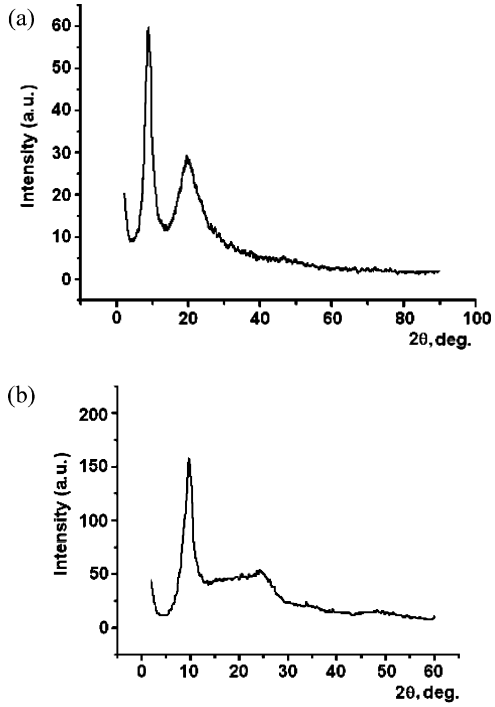

Figure 2. XRD Patterns of b-PDPHS (a) and PMPS (b).

In all cases, polyhydrosilanes show a low-angle peak around $2\theta = 9$ deg. The corresponding calculated D value, within 9.02−9.57 Å, was assigned to the distance between the main σ-conjugated polydiphenylsilyl chains as in conjugated aromatic polymers that have long chains disposed in ordered conformations.[12−14] The presence of the second peak around $2\theta = 20$ deg suggests that a second component of the intermolecular packing must be considered. This component corresponding to a calculated distance $d = 4.5$ Å should be understood by taking into account previous works which present polysilanes as a collection of fragmented helical segments.[11] According to this cholesteric hard core model, poly(diphenylhydrosilane)s take a long range ordered conformation defined by the helical pitch D and diameter d (Figure 3).

In the same position, the XRD pattern for PMPS (Figure 2b) shows only a broad irregular signal due to the amorphous halo of the polymer.

Methylhydrosilyl Chemical Transformations. Further analysis by DSC thermal scanning confirmed the higher flexibility of polyhydrosilanes due to the methylhydrosilyl segments, showing a strong variation of the T_g values proportional to the Si−H group content (Table 1 and Figure 4). Furthermore, the DSC profile of polyhydrosilanes revealed an intriguing exothermic peak within 100−135 °C. The TGA analysis performed in air as well as under nitrogen atmosphere (Supporting Information, TGA analysis) showed that the thermal decomposition of the polyhydrosilanes starts above 350 °C in all cases. This temperature is higher than the one mentioned in previous works.[15] The shape of the DSC exothermic peak and its location below the decomposition temperature, in the proximity of the T_g, indicate that this transition should be the result of some chemical transformation within the methylhydrosilyl segments which takes place without measurable weight loss probably by elimination of small molecules and/or by structural rearrangements into more thermally stable products. These processes could produce morphological changes on the polymer film surface. Therefore, further investigations were made by polarized light microscopy (PLM) thermal scanning. This method showed that small birefringent particles were formed within the liquefied polymer drops during the melting process of a-PDPHS and b-PDPHS. The process was irreversible and stopped after 5−10 min.

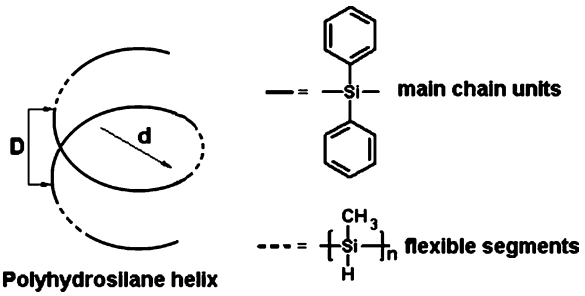

Figure 3. Formal representation of the polyhydrosilane helix conformation.

Table 1. Thermal Analysis of Polysilanes[a]

sample data	PMPS	PDPHS		
M_r		1/1	1/7	1/20
T_1, °C	388, 230[b]	316, 330[b]	358, 250[b]	360, 250[b]
T_2, °C		465, 540[b]	466, 470[b]	466
T_g, °C	88	64	85	85
exo peak, °C		101	135	135
endo peak, °C		131	150	150

[a] Mr = molecular ratio as prescribed; T_1 = temperature corresponding to the first decomposition peak; T_2 = temperature corresponding to the second decomposition peak; T_g = glass transition temperature; [b] Measured in nitrogen;

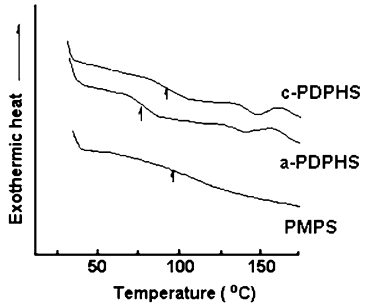

Figure 4. DSC profile of polysilanes.

The number of these particles increased with temperature and Si−H content but they were also detected when the films were prepared by dip-coating at room temperature. This indicates that the particle formation should start at even earlier stages of the polymer synthesis (Figure 5).

In the case of a polyhydrosilane with an extremely low concentration in Si−H groups as c-PDPHS, the particles attain nanometric dimensions and could be seen only by the Tyndall scattering light effect as blue colored large areas (Figure 6b). PMPS homopolymer was studied by the same procedures and

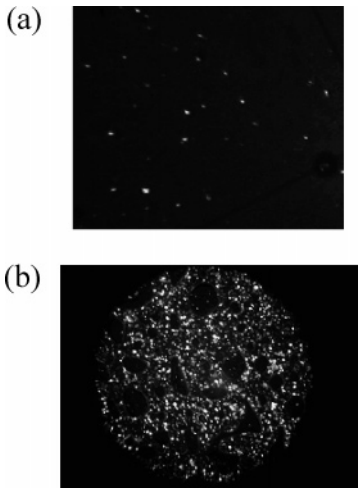

Figure 5. PLM images of a-PDPHS: (a) at room temperature; (b) after melting.

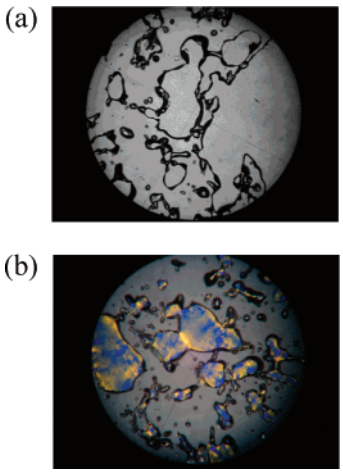

Figure 6. Microscopy images of c-PDPHS: (a) nonpolarized light; (b) polarized light.

in every case appeared to be an isotropic amorphous material within the scanned temperature range. Slow cooling of the melted polymer did not produce any birefringence.

These results suggest that the presence of methylhydrosilyl segments in polyhydrosilanes is related to intriguing chemostructural processes that lead to the formation of solid birefringent particles. These processes involve only part of the reactive centers located inside the methylhydrosilyl segments and have a limited extent.

The particles were further analyzed in order to determine their chemical structure and dimension.

AFM topographic analysis was performed on PDPHS and PMPS previously annealed to the melting temperature following the same procedure as in PLM experiments (Figure 7). In addition, images of the cantilever landing area were registered by the video-scan camera attached to the AFM unit. The film surface analysis shows randomly dispersed droplike structures (DL) and emerging solid particles (Figure 7, 8b; Supporting Information Figure S2). Annealing to the melting temperature leads to intermigration of these structures and the formation of small associations (Supporting Information Figure S3). The strange surface morphology of the films can be related to the previously presented DSC exotherms. Therefore, at the corresponding temperature, part of the methylhydrosilyl groups could participate to Kumada-like rearrangements with formation of embedded cross-linked polycarbosilane structures,[16] appearing

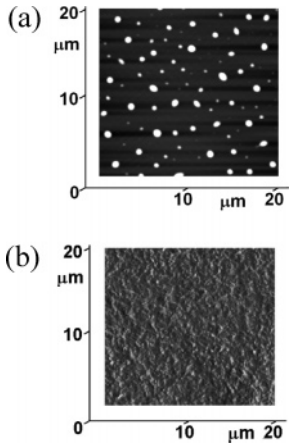

Figure 7. AFM images at 20 μm: c-PDPHS (a); PMPS (b).

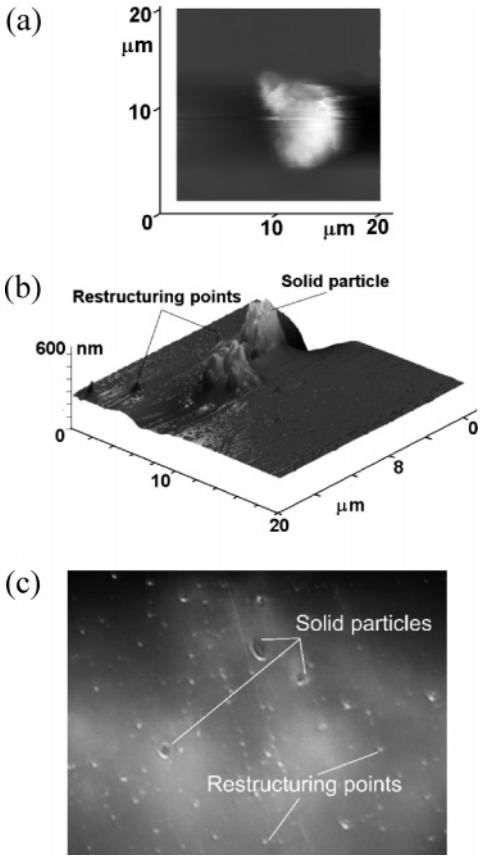

Figure 8. (a, b) AFM images of a solid particle on the film surface at 20 μm; (c) video scan picture of the landing area.

like droplike defects (DL) at the cross-linking points (Figure 8b,c).

These processes are sustained by the neighboring Si−H highly reactive centers which ensure a local propagation of the chemical reactions and finally freeze in various moments of development embedding a nanometric DL structure covered by the thick polymer film or emerging through it as a solid particle. Neither of these structures could be seen on the surfaces of PMPS homopolymers films (Figure 7b).

Information concerning the nature of the particles was obtained by XPS analysis.[17] The survey spectra of b-PDPHS and PMPS revealed the Si 2p, Si 2s, C 1s, and O 1s photoelectron lines. Comparative valence band and Si 2p core level spectra are presented in Figure 9.

In the case of the PMPS structure an estimate of the Si 2p binding energy (BE) in the bonding environment of (−Si(C_6H_5)-

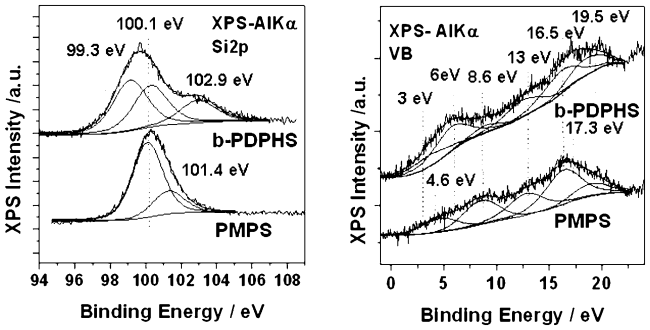

Figure 9. Comparative XPS Si 2p and valence band spectra of b-PDPHS and PMPS.

$(CH_3)-)_n$ was obtained from the group shift scheme proposed by Gray et al.[18] The experimentally observed BE = 100.1 eV (76% of the total Si 2p signal for PMPS) is very close to the scheme estimate of 100 eV for a Si atom coordinated by two other silicon atoms, a phenyl and a methyl group. According to the same scheme if one of the two silicon atoms is replaced by oxygen then the Si 2p peak would shift by another 0.95 eV resulting BE ~ 101 eV, a value that is close to the one experimentally observed at the second Si 2p component.

The C/Si and O/Si surface atomic ratios were calculated from the total intensities of the C 1s, Si 2p, and O 1s peaks, corrected by their atomic sensitivity factors 0.25, 0.27, and 0.66 respectively, and by the inelastic mean free paths of the photoelectrons in question assuming a model semiinfinite solid with homogeneous composition.[20] It was found that for PMPS C/Si = 7.1 is close to the nominal value for this structure. The O/Si atomic ratio was 0.43. If for the calculation of the oxygen content only the Si 2p peak at BE = 101.4 eV is considered, then O/Si(ox) = 2 suggesting that about 24% of the silicon atoms are coordinated to two oxygen atoms.

In the case of the PDPHS structure the C 1s spectrum consists of two main components one at BE = 284.6 eV (C−C, C═C, and C−H species) and one at 286.1 eV (C−O). A weak signal at the high BE side of the main peak (~292 eV), is the shake up satellite due to the phenyl groups.[19] The Si 2p spectrum of b-PDPHS contains three components at BE's 99, 100, and 102.9 eV. The peak at 99 eV represents elemental Si and its intensity is about 32.5% of the total Si 2p signal. The component at 102.9 eV represents partially oxidized Si atoms (27%). The O/Si surface atomic ratio is calculated to be 0.82. If only the Si 2p peak with BE = 102.9 is considered then the calculated O/Si-(ox) = 3.5 shows that part of the oxygen detected here is bonded directly to C atoms. The C 1s spectrum of b-PDPHS consists of only one component at 284.6 eV (C−C). The surface atomic ratio C/Si = 10.9 calculated taking into account the total C 1s and Si 2p signals is close to 10.6, which is the nominal value for a molar ratio $Ph_2Si/MeHSi$ = 7/1. The slight difference is probably due to surface contamination of the sample by residual graphitic-like carbon species.

The valence band region of samples b-PDPHS and PMPS was analyzed with mixed G−L components each one having fwhm = 4 eV. Comparison of the two spectra reveals that at b-PDPHS an additional peak appears at BE = 6 eV that can be attributed to Si−Si bonds.[21] This peak is very prominent in agreement with the Si 2p spectrum that indicates the existence of elemental Si. The peak at 19.5 eV assigned to −C−C− bonds from phenyl groups[21] is more prominent at b-PDPHS. The peak at 4.6 eV (sample PMPS) has been shifted toward lower BE's (closer to the Fermi level) in the case of b-PDPHS (BE = 3 eV).

Scheme 1. Formation of Elemental Silicon within Polyhydrosilane

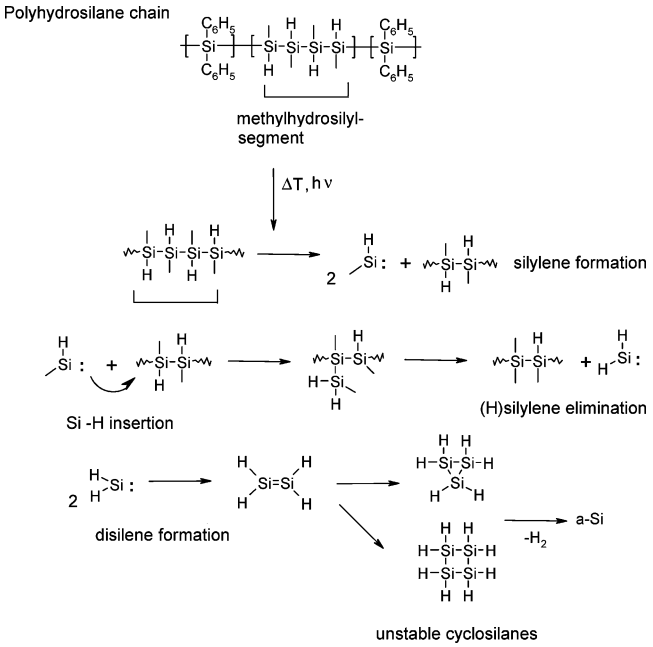

This enrichment in silicon was previously observed only when polysilanes had been exposed to intensive irradiation with high-energy UV light and was attributed to photodecomposition of the $-Si-CH_3$ bond.[22] The high instability of the enchained hydrogen substituted silicon atoms in linear or cross-linked structures as in polymethylsilane (PMS) has been previously reported.[23−27]

To explain the elemental silicon formation within polyhydrosilanes one should consider the synthesis stage when highly reactive silylene intermediates appear as a result of both halogen metal exchange during the Wurtz−Fittig-like condensation or thermophotolytic scission of the already formed methylhydrosilyl segments[28] (Scheme 1). Silylenes are subsequently inserted within the relatively week Si−H bond, by the initial formation of a donor−acceptor complex followed by a 1,2-atom shift.[29−31] This reaction leads to the appearance of relatively unstable carbohydridosilane branching centers attached to the silicon atoms in the immediate neighborhood of the Si−H reactive groups. These structures create local conformational distortions and could participate in Kumada rearrangements with cross-linking of the polysilane chains leading to formation of the embedded DL structures visible on the polyhydrosilanes film surface. Because of the complex action of the highly reactive silylene, the insertion reaction could take also a different course by elimination of the dihydrosilylene[32] and formation of unstable disilene and cyclic oligosilanes through dimerization.[33] These last structures containing only silicon and hydrogen atoms could generate elemental silicon as solid particles mounted within the polymeric matrix.[34,35]

Conclusions

The enclosure of methylhydrosilyl fragments within the poly-(diphenylsilane) chain causes major chemostructural effects. The coupling of the stiff diphenylsilyl segments through methylhydrosilyls eliminates the internal conformational tensions allowing the rearrangement of the polysilane structure with the formation of an ordered helical conformation. The decrease of the chain fractioning frequency allows the polydiphenylsilyl segments to reach a higher conjugative dimension improving the symmetry of the emissive electronic transitions.

On the other side, the chemical processes involving the participation of the Si−H groups cause the formation of elemental silicon particles. The linear methylhydrosilyl structure manifests a high structural instability due to the presence of methylhydrosilylene reactive species in the earlier stages of the synthesis process. Adjustment of the comonomer's molecular ratio allows the dimension control of these particles down to the nanometric level.

Exploitation of these intriguing properties of polyhydrosilanes opens new possibilities for applications aiming to the quantum dimension of optoelectronics.

Experimental Section

General Remarks. Diphenyldichlorosilane, $Cl_2Si(C_6H_5)_2$ (purum, >98%) and methyldichlorosilane, $CH_3(H)SiCl_2$ (purum, >98%) were purchased from Fluka and distilled prior to use.

Toluene and tetrahydrofuran (THF) were purchased from a commercial source and used after distillation over sodium wire.

Poly(methylphenylsilane) homopolymer (PMPS) was synthesized according to[9] $M_w = 62 \times 10^3$ g mol^{-1} and M_w/ Mn = 1.32. FTIR (KBr, cm^{-1}): 3020−3000 (C−Har), 2920 and 2850 (C−H), 1210 and 870 (Si−CH_3), 750 and 700 (Si−C), 470 (Si−Si). ^{1}H NMR ($CDCl_3$, δ ppm): 0.05−0.15 (3H, broad, −$SiCH_3$), 7.2−7.5 (6H, m, −SiC_6H_5). ^{13}C NMR ($CDCl_3$, δ ppm): −4.0 (−$SiCH_3$), 125.3−133.2 (−SiC_6H_5). UV−vis (λ_{max}, nm; ϵ, L·mol^{-1}·cm^{-1}): 280 (8000), 330 nm (15800).

Measurements. FTIR spectra were recorded with an FTS 40A Bio-Rad spectrometer at room temperature on KBr pellets. ^{1}H NMR and ^{13}C NMR spectra were recorded with a Bruker NMR instrument (model DRX 400 MHz). Chemical shifts are given in parts per million (ppm) without TMS as internal standard.

Gel permeation chromatography (GPC) experiments were carried out in THF solution at 30 °C, at a flow rate 1 cm^3/min using a Spectra Physics 8800 gel permeation chromatograph.

UV/vis spectra were recorded in chloroform solution using a Beckman Acta M4 spectrometer.

Steady-state fluorescence (FL) spectra were recorded in CH_3Cl solution (10^{-3} mol·L^{-1}) using a Perkin-Elmer Hitachi MPF 43B spectrofluorimeter operating with a 150 W Xe arc lamp at room temperature.

Thermogravimetric analysis (TGA) was performed in air on a MOM Paulik−Paulik−Erdey derivatograph at a 10 °C/min heating rate, then in nitrogen using a thermogravimetric cell Mettler 851e, at a heating rate 15 K/min.

Differential scanning calorimetry (DSC) measurements were carried out in a Mettler DSC12E calorimeter at a heating rate of 10 °C/ min, in air.

The polarized light microscopy (PLM) study was made within 25−200 °C using the Euromex ME 2885 trinocular microscope equipped with an infrared controlled heating bench.

The atomic force microscopy investigations were carried out using the AFM microscope Solver PRO-M, NT−MDT. The measurements were done in air using the taping mode of the AFM, employing as probes NSG10/Au silicon cantilevers of typical force constant $K_N = 11.5$ N/m.

The X-ray photoelectron spectrometry (XPS) measurements were carried out in an ultrahigh vacuum (UHV) system, which has been described in detail elsewhere.[10,17] The unmonochromatized Al Kα line at 1486.6 eV and constant analyzer pass energy of 97 eV, giving a full width at half-maximum (fwhm) of 1.7 eV for the Au $4f_{7/2}$ peak, were used in all XPS measurements. The XPS core level spectra were analyzed with a fitting routine that decomposes each spectrum into individual mixed Gaussian−Lorentzian (G−L) peaks after a Shirley background subtraction. The error in the XPS core level peak positions for a good signal-to-noise ratio is ±0.05 eV. The binding energy (BE) scale was calibrated by assigning the main C 1s peak at 284.6 eV.

The polymers in the form of powder were pressed in pellets under ambient atmosphere, before their introduction to the UHV system.

X-ray diffraction analysis was performed using a Bruker AxS D8 Advance X-ray difractometer equipped with a copper anode tube (Cu Kα, 1.5406 Å) operated at 36 kV/ 20 mA, Nickel filter, θ/θ base goniometer and scintillation detector. The data were processed automatically by the Diffrac Plus XRD Commander software of the instrument.

Synthesis of Polysilanes. The synthesis of the poly[diphenylsilane-*co*-methyl(H)silane] copolymers with a variable content of Si−H groups and narrow molecular weights distribution was performed through the homogeneous coupling of diphenyldichlorosilane with calculated amounts of methyl(H)dichlorosilane[9] (Supporting Information) The composition of the poly[diphenylsilane-*co*-methyl(H)silane] (PDPHS) was controlled by selection of specific $CH_3HSiCl_2/(C_6H_5)_2SiCl_2$ monomers with ratios 1/1 (a-PDPHS), 1/7 (b-PDPHS) and 1/20 (c-PDPHS).

GPC analysis: a-PDPHS, $M_w = 50.2 \times 10^3$ g mol^{-1} ($M_w/M_n = 1.20$); b-PDPHS, $M_w = 45.1 \times 10^3$ g mol^{-1} ($M_w/M_n = 1.12$); c-PDPHS, $M_w = 48.0 \times 10^3$ g mol^{-1} ($M_w/M_n = 1.18$).

Spectroscopic Analyses. FTIR (a-PDPHS, KBr, cm^{-1}): 3070−3000 (C−Har), 2980 and 2860 (C−H), 2080 (Si−H), 1455 and 1100 (Si−C_6H_5), 1250 and 880 (Si−CH_3), 750 and 705 (Si−C), 460 (Si−Si). ^{1}H NMR (a-PDPHS, δ ppm, $CDCl_3$): 0.15, 0.65 (3H, −$SiCH_3$), 3.80 (1H, −SiH), 7.3−7.6 (12H, −SiC_6H_5). ^{13}C NMR (δ ppm, $CDCl_3$): −8.2, −0.8 (−$SiCH_3$), 126.5−135.7 (−SiC_6H_5). UV−vis (λ_{max}, nm; ϵ, L·mol^{-1}·cm^{-1}): 285 (6500), 352 (14800), a-PDPHS; 280 (6600), 350 (14300), b-PDPHS; 283 (6800), 350 (14500), c- PDPHS; 280 (6000), 340 (14700), PMPS (Supporting Information Figure S1).

FL (λ_{exc}, nm): 367.5, PDPHS; 355.0, PMPS (Figure 1).

XRD (2θ, deg): 9.79 ($D = 9.02$ Å), 20.34 ($d = 4.36$ Å), a-PDPHS; 8.92 ($D = 9.90$ Å), 20.95 ($d = 4.23$ Å), b-PDPHS; 9.23 ($D = 9.57$ Å), 19.47 ($d = 4.55$ Å), c-PDPHS; 9.78 ($D = 9.03$ Å), PMPS, (Figure 2).

TGA onset decomposition temperatures in air and nitrogen (Supporting Information) and the DSC scanning profiles are presented in Table 1, Figure 4.

PLM was used to investigate the optical properties of polysilanes within 50−200 °C. The samples were prepared as powders and by dip-coating at room temperature from a 2% solution in chloroform and vacuum-dried 48 h at 40 °C. Images of the polymers surfaces are shown in (Figure 5 and 6).

AFM analyses were performed on PDPHS and PMPS films prepared by dip-coating from a 2% solution in chloroform and vacuum-dried 48 h at 40 °C. The polymer samples were previously annealed to the melting temperature as in PLM experiments. The topographic images are shown in Figure 7 and 8 and Supporting Information (Figure S2 and S3).

The XPS analysis was performed on a-PDPHS and b-PDPHS copolymers. The results were compared with those obtained for the Si−H free homopolymer (PMPS). XPS spectra showing the core level Si 2p photoelectron lines of the samples are presented in Figure 9.

Acknowledgment. The authors express thanks to the Romanian Ministry of Education, Matnantech Project No. 36/ 2005, for supporting this work.

Supporting Information Available: Text giving experimental details, including synthesis procedure, and figures showing the UV−vis spectra and AFM images. This material is available free of charge via the Internet at http://pubs.acs.org.

References and Notes

(1) Takagi, H.; Ogawa, H.; Yamazaki, Y.; Ishizaki, A.; Nagakiri, T. *Appl. Phys. Lett.* **1990**, *56*, 2379−2380.
(2) Goldstein, A. N. *Appl. Phys. A: Mater. Sci. Process.* **1996**, *62*, 33−37.
(3) Furukawa, S.; Miyasato, T. *Superlattices Microstruct.* **1989**, *5*, 317−320.
(4) Castro, D. T.; Ying, J. H. *Mater. Sci. Eng. A* **1995**, *204*, 65−70.

(5) (a) Bhargava, R.N. U.S. Pat. 5,446,286, 1995. (b) Hasan, M.A.; Elqaq, D.H. U.S. Pat. 6,764,368, 2004.
(6) (a) Yajima, S.; Hayashi, J.; Omori, M.; Okamura, K. *Nature (London)* **1976**, *261*, 683−685. (b) Baney, R. H.; Gaul, J. H., Jr.; Hilty, T. K. *Organometallics* **1983**, *2*, 859−864. (c) Yajima, S.; Hayashi, J.; Omori, M. *Chem. Lett.* **1975**, 931−934. (d) West, R.; David, L. D.; Djurovich, P. I.; Yu, H.; Sinclair, R. *Ceram. Bull.* **1983**, *62*, 899−903. (e) West, R.; David, L. D.; Djurovich, P. I.; Stearley, K. L.; Srinivasan, K. S. V.; Yu, H. *J. Am. Chem. Soc.* **1981**, *103*, 7352−7354.
(7) Pola, J.; Parsons, J. P.; Taylor, R. *J. Organomet. Chem.* **1995**, *489*, 9−11.
(8) Baggott, J. E.; Frey, H. M.; Lightfoot, P. D.; Walsh, R. *Chem. Phys. Lett.* **1986**, *125*, 22−26.
(9) (a) Sacarescu, G.; Sacarescu, L.; Ardeleanu, R.; Kurcok, P.; Jedliński, Z. *Macromol. Rapid Commun.* **2001**, *22*, 405−408. (b) Sacarescu, G.; Voiculescu, N.; Marcu, M.; Sacarescu, L.; Ardeleanu, R.; Simionescu, M. *J. Macromol. Sci.—Pure Appl. Chem.* **1997**, *A34*, 509−516.
(10) Fujiki, M. *J. Am. Chem. Soc.* **1994**, *116*, 6017−6018.
(11) Fujiki, M.; Koe, J. R.; Terao, K.; Sato, T.; Teramoto, A.; Watanabe, J. *Polym. J.* **2003**, *35*, 4, 297−344.
(12) (a) McCullough, R. D.; Lowe, R. D. *J. Chem. Soc. Chem. Commun.* **1992**, 70−72. (b) McCullough, R. D.; Tristam-Nagle, S.; Willams, S. P.; Lowe, R. D.; Jayaraman, M. *J. Am. Chem. Soc.* **1993**, *115*, 4910−4911. (c) McCullough, R. D. *Adv. Mater.* **1998**, *10*, 93−116.
(13) (a) Chen, T.-A.; Rieke, R. D. *J. Am. Chem. Soc.* **1992**, *114*, 10087−10088. (b) Chen, T.-A.; Wu, X.; Rieke, R. D. *J. Am. Chem. Soc.* **1995**, *117*, 233−244.
(14) Politis, J. K.; Nemes, J. C.; Curtis, M. D. *J. Am. Chem. Soc.* **2001**, *123*, 2537−2547.
(15) (a) Horiguchi, R.; Onishi, Y.; Hayase, S. *Macromolecules* **1988**, *21*, 304−309. (b) Miller, R. D.; Michl, J. *Chem. Rev.* **1989**, *89*, 1359−1410. (c) Pan, L.; Zhang, M.; Nakayama, Y. *Chem. Mater.* **1999**, *11*, 1326−1330.
(16) Kumada, M.; Tamao, K. *Adv. Organometal. Chem.* **1968**, *6*, 19−117.
(17) Siokou, A.; Ntais, S. *Surf. Sci.* **2003**, *540*, 379−388.
(18) Gray, R. C.; Carver, J. C.; Hercules, D. M. *J. Electron Spectrosc. Relat. Phenom.* **1976**, *8*, 343−357.
(19) Inagaki, N.; Hirao, H. *J. Polym. Sci., Part A: Polym. Chem.* **1986**, *24*, 595−602.
(20) Briggs, D.; Seah, M. P. *Practical Surface Analysis*, 2nd ed.; Wiley: New York, 1996; Vol. 1.
(21) (a) Kuroki, S.; Endo, K.; Maeda, S.; Chong, D. P.; Duffy, P. *Polym. J.* **1998**, *30*, 142−148. (b) Yeh, J. J.; Lindau, I. *At. Data Nucl. Data Tab.* **1985**, *32*, 1−155.
(22) (a) Trefonas, P.; West, R.; Miller, R. D. *J. Am. Chem. Soc.* **1985**, *107*, 2737−2742. (b) Azinovi, D.; Bravo-Zhivotovskii, D.; Bendikov, M.; Apeloig, Y.; Tumanskii, B.; Veprek, S. *Chem. Phys. Lett.* **2003**, *374*, 257−263.
(23) (a) Seyferth, D.; Wood, T. G.; Tracy, H. J.; Robison, J. L. *J. Am. Ceram. Soc.* **1992**, *75*, 1300−1302. (b) Seyferth, D.; Tracy, H. J.; Robison, J. L. US Pat. 5,204,380, 1993. (c) Seyferth, D.; Yu, Y-F. In *Design of New Materials*, Cocke, D. L., Clearfield, A., Eds.; Plenum Press: New York, 1987; p 79.
(24) Seyferth, D.; Lang, H. *Organometallics* **1991**, *10*, 551−558.
(25) (a) Mu, Y.; Harrod, J. F. In *Inorganic and Organometallic Oligomers and Polymers, IUPAC 33rd Symposium on Macromolecules*; Harrod, J. F., Laine, R. M., Eds.; Kluwer Publ.: Dordrecht, The Netherlands, 1991; p 23. (b) Harrod, J. F. In *Inorganic and Organometallic Polymers with Special Properties*; NATO ASI Ser. E; Laine, R. M., Eds.; Kluwer Publ.: Dordrecht, The Netherlands, 1991; Vol. 206, p 87. (c) Xin, X.; Aitken, C.; Harrod, J. F.; Mu, Y. *Can. J. Chem.* **1990**, *68*, 471−476. (d) Liu, H. Q.; Harrod, J. F. *Organometallics* **1992**, *11*, 822−827. (e) He, J.; Liu, Q.; Harrod, J. F.; Hynes, R. *Organometallics* **1994**, *13*, 336−343.
(26) Kobayashi, T.; Sakakura, T.; Hayashi, T.; Yumura, M.; Tanaka, M. *Chem. Lett.* **1992**, 1157−1160.
(27) (a) Zhang, Z.-F.; Babonneau, F.; Laine, R. M.; Mu, Y.; Harrod, J. F.; Rahn, J. A. *J. Am. Ceram. Soc.* **1991**, *74*, 670−673. (b) Zhang, Z-F.; Mu, Y.; Laine, R. M.; Babonneau, F.; Harrod, J. F.; Rahn, J. A. In *Inorganic and Organometallic Oligomers and Polymers, IUPAC 33rd Symposium on Macromolecules*; Harrod, J. F., Laine, R. M., Eds.; Kluwer Publ.: Dordrecht, The Netherlands, 1991; pp 127−146.
(28) Wilberg, N.; Niedermayer, W. *J. Organomet. Chem.* **2001**, *628*, 57−64.
(29) Helmer, B. J.; West, R. *Organometallics* **1982**, *1*, 1458−1463.
(30) (a) Steele, K. P.; Tzeng, D.; Weber, W. P. *J. Organomet. Chem.* **1982**, *231*, 291−298. (b) Masamune, S. In *Silicon and Germanium Double Bond and Polycyclic Ring Systems, Silicon Chemistry*; Corey, E. R., Corey, J. Y., Gaspar, P. P., Eds.; Ellis Horwood: New York, 1988. Chapter 25, p 257.
(31) Conlin, R. T.; Netto-Ferreira, J. C.; Zhang, S.; Scaiano, J. C. *Organometallics* **1990**, *9*, 1332−1334.
(32) Walsh, R. In *Chemistry of Organic Silicon Compounds, Thermochemistry*; Patai, S., Rappoport, Z., Eds.; Wiley: Chichester, U.K., 1989; Vol. 1, Chapter 5, p 371.
(33) (a) Nakadaira, Y.; Kobayashi, T.; Otsuka, T.; Sakurai, H. *J. Am. Chem. Soc.* **1979**, *101*, 486−487. (b) West, R. *Angew. Chem.* **1987**, *26*, 1201−1302.
(34) Narisawa, M.; Tanno, H.; Ikeda, M.; Iseki, T.; Mabuchi, H.; Okamura, K.; Oka, K.; Dohmaru, T.; Kim, D. P. *J. Ceram. Soc. Jpn.* **2006**, *114*, 558−562.
(35) Seyferth, D.; Lang, H.; Sobon, C. A.; Borm, J.; Tracy, H. J.; Bryson, N. *J. Inorg. Organomet. Polym.* **1992**, *2* (1), 59−77.

MA071853F